Probing Amino Acid Interaction with a Polystyrene Nanoparticle Surface Using Saturation-Transfer Difference (STD)-NMR

*Yunzhi Zhang and Leah B. Casabianca**

Department of Chemistry, Clemson University, Clemson, SC, USA.

AUTHOR INFORMATION

Corresponding Author

*lcasabi@clemson.edu

ABSTRACT

The interaction between individual amino acids and the surface of carboxylate-modified polystyrene nanoparticles in solution was studied using Saturation-Transfer Difference (STD)-NMR. Individual amino acids were screened for nanoparticle binding using an STD-NMR experiment at a fixed saturation time, and STD buildup curves were measured for those amino acids that exhibited significant STD difference signals in the initial screening. The strongest STD effects were measured for protons of aromatic side chains, with relatively weaker effects observed for protons in long-chain aliphatic and positively-charged side chains. This indicates that there are several modes of binding to these polystyrene nanoparticles: electrostatic attraction between the negatively-charged surface of the carboxylate-modified polystyrene nanoparticle and positively-charged amino acids, hydrophobic effects between long aliphatic side chains and the nanoparticle surface, and pi-pi interactions between aromatic amino acids and aromatic groups in styrene. This information can be used in future studies to predict and understand interactions between nanoparticle surfaces and specific amino acid residues in small peptides and proteins.

TOC GRAPHICS

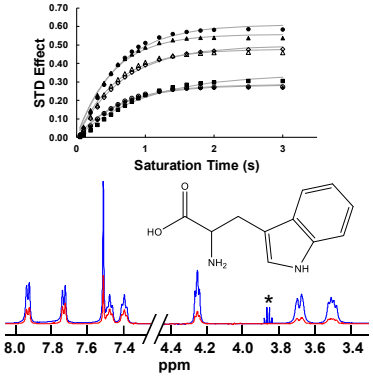

KEYWORDS pi-pi interactions, tryptophan, phenylalanine

Interactions between nanoparticle surfaces and biological molecules are relevant to many areas of nanomedicine and human health.[1-7] A molecular-level understanding of the interactions between peptides or proteins and nanoparticle surfaces will be essential to optimizing biocompatible coatings for nanoparticles to be used as therapeutic and diagnostic devices,[8-10] as well as understanding the fate of nanoparticles that enter the body unintentionally.[11,12] Since hydrophobic residues are typically buried inside a protein's interior, when a peptide binds to a hydrophobic nanoparticle surface, it will presumably change its shape in order to maximize favorable hydrophobic interactions with the nanoparticle surface.[13] A change in structure can result in a change in biological function of the protein,[14-17] so having techniques to examine the structure of peptides and proteins adsorbed on a nanoparticle surface is crucial. Epitope mapping, or identification of the specific amino acid residues that interact with a particular nanoparticle surface, is not trivial.[15-18] Nuclear Magnetic Resonance (NMR) is the analytical method of choice for molecular-level structure determination in most situations. Large particles such as nanoparticles present difficulties in solution-state NMR, due to their slow molecular tumbling and resulting short T_2 relaxation times and broad peaks. However, several solution-state NMR studies[19-23] have examined binding between peptides and nanoparticles in situ. Ligand-detected NMR techniques, which do not rely on being able to observe the large nanoparticle in solution, are especially promising in this field. One such ligand-detected technique is Saturation-Transfer Difference (STD)-NMR.

The STD-NMR method[24-27] has been used extensively in the drug delivery field to screen drug candidates for binding to a protein receptor.[28] The STD experiment has the advantage that large receptor proteins, which are too big to be observed in solution-state NMR, can be studied. In addition to being a screening technique, the STD-NMR experiment can also be used to determine

binding constants[29] and for epitope mapping - determining which protons in the ligand are closer to the receptor in the bound configuration.[25]

An STD-NMR experiment consists of collecting a set of two spectra. The first is a reference "off-resonance" spectrum in which saturation is performed by irradiating the sample at a frequency that is far from where either the ligand or receptor protons resonate (40 ppm was used in the current work). The second spectrum is an "on-resonance" spectrum in which saturation is performed at a frequency that is far from the ligand resonances, but in a position in which the broad peaks of the receptor protons are expected (12 ppm was used in this work). Ligands that interact with the receptor during the saturation time will have some of the saturation transferred from the receptor protons to their protons through the nuclear Overhauser effect. This will lead to a decrease in the intensity of the NMR signal corresponding to those ligand protons. Ligands that do not interact with the receptor will have the same NMR intensity in the on- and off-resonance spectra. An STD difference spectrum, obtained by subtracting the on-resonance spectrum from the off-resonance spectrum, therefore contains signal from only those ligands that interact with the receptor during the saturation time. The degree of interaction can be quantified using the STD Effect, which is defined as the STD difference intensity divided by the reference intensity.[25]

Previously, we[30,31] and others[32] have shown that STD-NMR can be used to determine binding constants and binding epitopes for small molecules that interact with the surface of organic nanoparticles that contain a dipolar-coupled network of proton spins. In the current work, we aim to facilitate the eventual study of small peptides binding to nanoparticle surfaces by first screening individual amino acids for binding to a negatively-charged polystyrene nanoparticle surface. The polystyrene nanoparticles we use here have been used previously as model nanoparticles for studying the protein corona,[33] nanoparticles crossing in vitro blood-brain

barriers,[34] the mechanism of endocytotic uptake of nanoparticles into endothelial cells and macrophages,[35] and the toxicity of nano-scale plastic in brine shrimp.[36] Due to the variety of chemical functional groups present in amino acid side chains, we developed insight into different possible binding modes for carboxylate-modified polystyrene nanoparticles.

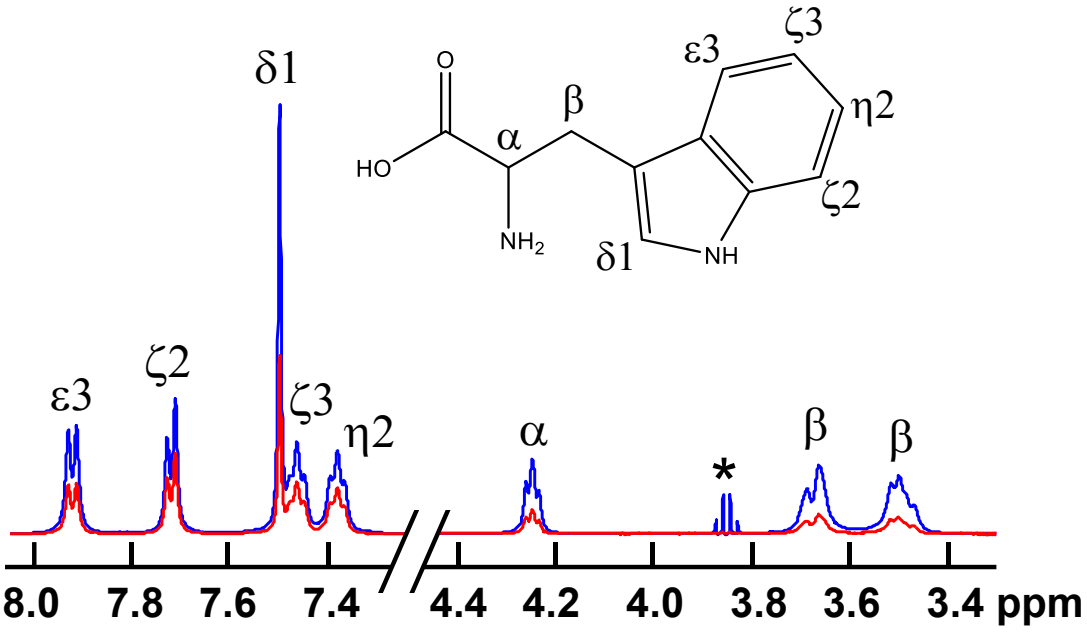

Figure 1. STD reference (blue) and difference (red) spectrum for tryptophan in the presence of 20-nm polystyrene beads. For this experiment, the recycle delay was 12 s. Peak assignments are shown corresponding to those labeled on the chemical structure of tryptophan in the inset. * indicates ethanol impurity present in the polystyrene bead suspension.

We first screened all amino acids for interaction with the polystyrene nanoparticle surface using a relatively long saturation time of 10 s. An example STD reference spectrum and STD difference spectrum are shown for tryptophan in Figure 1. Results of these initial screening experiments for all amino acids are listed in Table 1.

Table 1. STD Effects at 10 s Saturation Time

Amino Acid	STD Effect	Amino Acid	STD Effect
Gly	0.000	Pro	0.003
Ala	0.000	Phe	0.195
Ser	0.001	Trp	0.572
Thr	0.000	Asn	-0.001
Cys	0.001	Gln	0.000
Val	0.004	His	0.197
Leu	0.019	Lys	0.017
Ile	0.016	Arg	0.060
Met	0.017		

When the amino acid contains more than one proton peak, the STD effect for the proton having the largest STD effect is listed. The error on these values is estimated to be ± ≤0.004. This error was estimated by performing five different experiments on the same tryptophan sample, phasing each resulting spectrum two ways (manually and automatically), and using three different reasonable limits of integration. The standard deviation of the resulting 30 STD values for each tryptophan peak was 0.001-0.004. Tyrosine, aspartic acid, and glutamic acid were not tested due to their low solubility in unbuffered D_2O. A recycle delay of 12 s was used for these experiments.

From the data in Table 1, we can identify trends in the amino acids that bind to the nanoparticle surface. Most amino acids do not exhibit significant interactions with the nanoparticle surface, as indicated by STD effects of 0.004 or less. These include aliphatic amino acids with short side chains (glycine, alanine, and valine), amino acids with polar uncharged groups (serine, threonine, asparagine, and glutamine), proline and cysteine.

Among the amino acids that do exhibit STD effects when interacting with a polystyrene nanoparticle surface are amino acids with positively-charged side chains: arginine and lysine. This is expected since the carboxylate-modified surface is negatively charged. Leucine, isoleucine, and methionine, which have long aliphatic side chains, also exhibit small but

significant STD effects. The largest STD effects, however, are observed for the aromatic amino acids histidine, phenylalanine and tryptophan. Note that tryptophan was studied at a lower concentration than the other amino acids due to its low solubility, so the ligand:receptor ratio for tryptophan was lower than that of the other samples. This also contributes to the high STD effect observed for tryptophan, because a low ligand:receptor ratio allows a greater fraction of ligand molecules to interact with the nanoparticle surface during the saturation time.

Based on these trends, functional groups that are responsible for binding to the nanoparticle surface can be identified. The observed STD effects for positively-charged, long aliphatic, and aromatic amino acids indicate that there may be several modes of binding to a carboxylate-modified polystyrene nanoparticle surface. Positively-charged functional groups are attracted to the negatively-charged carboxylate surface, resulting in relatively weak but observable interactions. Long-chain aliphatic amino acids may interact with the polystyrene surface due to hydrophobic effects. The last mode of binding likely involves pi-pi interactions between aromatic functional groups and the aromatic groups of the polystyrene, leading to strong binding between aromatic amino acids and polystyrene nanoparticles. This is in agreement with previous studies of phenylalanine interacting with a polystyrene surface using sum-frequency generation (SFG) spectroscopy.[37,38] An angle between the phenylalanine aromatic ring and polystyrene surface of approximately 70° was found, which is indicative of pi-pi interactions.

All other things being equal, a larger STD effect indicates stronger binding, but the STD effect is influenced by many factors. These include the saturation time, ligand:receptor ratio, relaxation rates of the ligand and receptor protons involved, and on/off binding rate constants.[39] Angulo *et al.*[29,40] have suggested that the initial slope of the STD buildup curve can be a better measure of the relative strength of binding than the STD effect at one particular saturation time, since it

alleviates complications due to ligand re-binding as well as differential relaxation of different protons during the saturation time. For the eight amino acids with observable STD effects, we have measured the STD buildup curves and found the initial slopes by nonlinear least-squares fitting.

The STD buildup curves for the aromatic amino acids, along with the chemical structure of each amino acid, are shown in Figure 2. Also shown in Figure 2 are chemical structures of the aromatic amino acids with the percent of the largest initial slope of the STD buildup curve listed next to each proton. The proton with the largest initial slope (100%) is always located in the aromatic part of the side chain, and the initial slopes are generally higher for the aromatic protons than the α and β protons for each amino acid. This indicates that the aromatic groups are responsible for the interaction with the nanoparticle surface. STD buildup curves for the remaining amino acids with a substantial STD effect in the initial screening experiments are shown in Figure S1 of the supporting information. For the positively-charged amino acids, the proton with the highest initial slope is located near the positive charge in the side chain, indicating that electrostatic effects may be responsible for binding in these cases. The initial slope of the STD buildup curve for each proton of all amino acids tested, with errors, are also listed in the supporting information, in Table S2.

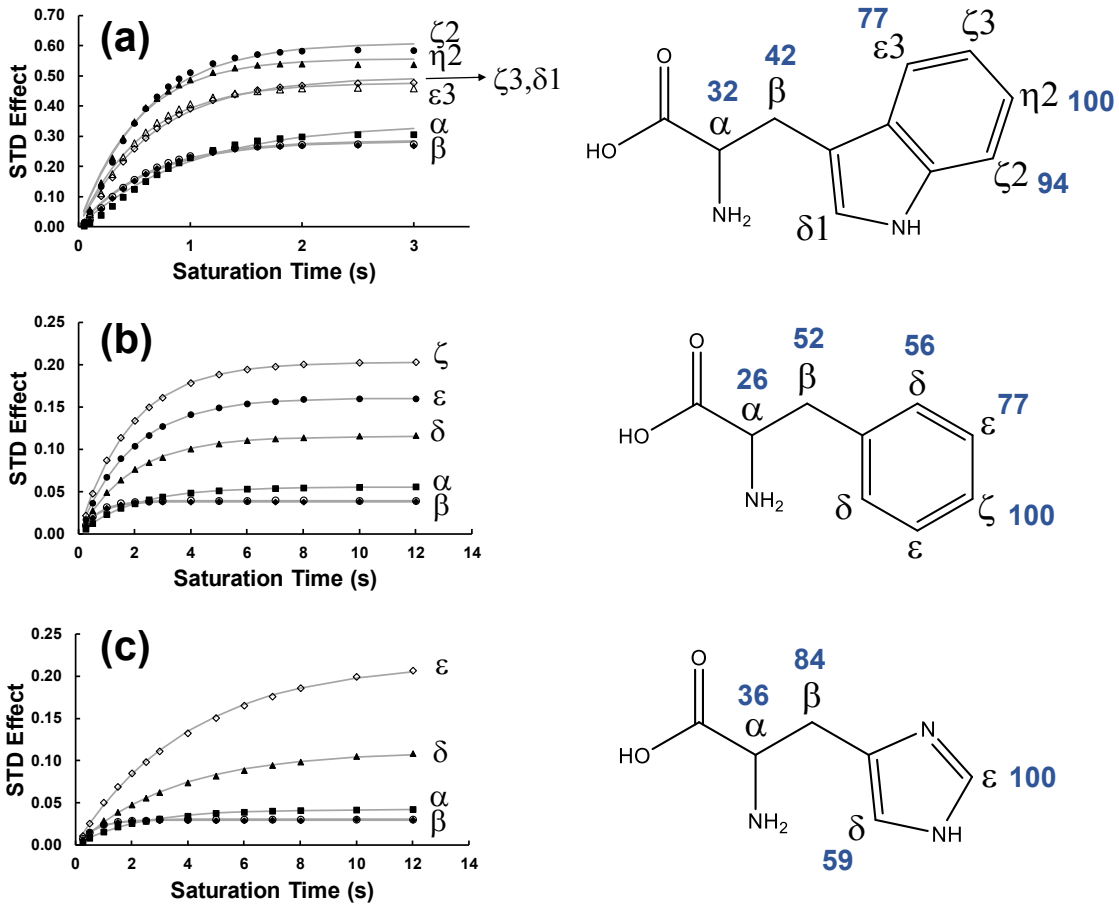

Figure 2. STD buildup curves for aromatic amino acids (a) tryptophan, (b) phenylalanine, and (c) histidine. Points are experimental STD effects and solid lines represent best fits from nonlinear least-squares fitting to the equation $S(t) = S_{max}(1 - e^{-kt})$ where S(t) is the STD effect at a saturation time t, S_{max} is the maximum STD effect, and k is a buildup time constant. Chemical structures are shown to the right of each buildup curve and are labeled with proton peak numbering scheme. The percent of the largest initial slope of the buildup curve is also listed in blue next to each proton on the chemical structure. When a percent value is not listed, it could not be determined due to peak overlap. For these experiments, recycle delays of 15 s were used for (b) and (c) and 12 s was used for (a). The two diastereotopic β protons were integrated separately, but their buildup curves overlap. The percent of the initial slope for the two β protons was averaged.

In conclusion, we have identified amino acids that interact with the surface of carboxylate-modified polystyrene nanoparticles and collected experimental evidence that there may be multiple binding modes for amino acids interacting with these nanoparticles. Through STD-NMR measurements and epitope mapping, we have observed that electrostatic effects can lead to relatively weak binding between amino acids with positively-charged side chains and the nanoparticle surface. Long-chain aliphatic amino acids also exhibit relatively weak binding, presumably due to hydrophobic effects. Aromatic amino acids exhibit comparatively stronger binding to the polystyrene nanoparticle surface, indicative of pi-pi interactions between the aromatic side chain of the amino acid and the phenyl rings in polystyrene. This work also further validates the use of STD-NMR to study binding between small molecule ligands and organic nanoparticles and provides insight into which amino acid residues in a peptide can be expected to interact with a nanoparticle surface.

Experimental Methods

L-amino acids (with the exception of D-phenylalanine) were purchased from Sigma-Aldrich (St Louis, MO) and used without further purification. Carboxylate-modified (CML) polystyrene latex spheres (20 nm, 4 % w/v suspension in water) were purchased from ThermoFisher Scientific (Waltham, MA, USA). Deuterium oxide (99.8 atom % D, Acros Organics) was purchased from Fisher Scientific, Inc. Millipore Milli-Q purified water was used for samples requiring H_2O.

Samples were made by dissolving each amino acid in D_2O, followed by addition of the polystyrene latex sphere suspension. For control samples, the same volume of H_2O was added in place of the polystyrene latex suspension. Samples were transferred to 5 mm OD NMR tubes

(Norell, Inc., Morganton, NC) for measurement. No buffer was used, as high salt concentrations can cause the beads to flocculate. The final pH of each sample was measured using an accumet AB150 pH meter with an accupHast MicroProbe glass body electrode. The final pH of each sample is listed in Table S1 of the supporting information. The reported pH values are those read directly from the pH meter, and were not corrected for the isotope effect. The final concentration of amino acid in all samples was 100 mM, with the exception of tryptophan, lysine, and arginine. For tryptophan, a final concentration of 35 mM was used due to the low solubility of tryptophan in pure D_2O. Lysine, arginine, and histidine samples were adjusted to a pH near 7 by addition of dilute HCl, resulting in final concentrations of 75 mM in the lysine sample and 80 mM in the arginine sample. Tyrosine, aspartic acid, and glutamic acid were not studied due to their low solubility in un-buffered D_2O. The final concentration of polystyrene beads in each sample was 550 nM. A 1D proton NMR spectrum of polystyrene beads alone is shown in Figure S2 of the supporting information.

All NMR experiments were performed on a 500 MHz Bruker Avance NEO NMR spectrometer equipped with a broadband Prodigy® nitrogen-cooled cryoprobe. The ^1H 90° pulse length was 12.0 μs. Saturation-transfer difference experiments were measured using the "stddiffesgp" pulse sequence[24] which incorporates excitation sculpting[41] for water suppression. On-resonance saturation was performed at 12.0 ppm and off-resonance saturation was performed at 40 ppm. 16 scans each (on-resonance and off-resonance) were collected for each experiment. A train of 50-ms Gaussian pulses at a power of 7.8 mW was used for saturation. A spectral width of 10 ppm and an acquisition time of 3 s was used. Recycle delays were 12-15 s as noted in the figure and table captions. All experiments were done at 298.0 K.

ASSOCIATED CONTENT

Supporting Information. The following files are available free of charge.

Final pH of each sample, STD buildup curves for amino acids not listed in Figure 2, initial slope of the STD buildup curve with errors for all amino acids, and 1D proton NMR of polystyrene beads. (.docx)

AUTHOR INFORMATION

Notes

The authors declare no competing financial interests.

ACKNOWLEDGMENT

LBC thanks the National Science Foundation (Grants CHE-1751529 and CHE-1725919) for support of this research.

REFERENCES

(1) Lynch, I.; Dawson, K. A. Protein-Nanoparticle Interactions. *Nano Today,* **2008**, *3*, 40-47.

(2) Mahon, E.; Salvati, A.; Baldelli Bombelli, F.; Lynch, I.; Dawson, K. A. Designing the Nanoparticle-Biomolecule Interface for "Targeting and Therapeutic Delivery." *J. Control. Release* **2012**, *161*, 164-174.

(3) Monopoli, M. P.; Åberg, C.; Salvati, A.; Dawson, K. A. Biomolecular Coronas Provide the Biological Identity of Nanosized Materials. *Nat. Nanotechnol.* **2012**, *7*, 779-786.

(4) Reidy, B.; Haase, A.; Luch, A.; Dawson, K. A.; Lynch, I. Mechanisms of Silver Nanoparticle Release, Transformation and Toxicity: A Critical Review of Current Knowledge and Recommendations for Future Studies and Applications. *Materials* **2013**, *6*, 2295-2350.

(5) Hu, Y.; Mignani, S.; Majoral, J.-P.; Shen, M.; Shi, X. Construction of Iron Oxide Nanoparticle-Based Hybrid Platforms for Tumor Imaging and Therapy. *Chem. Soc. Rev.* **2018**, *47*, 1874-1900.

(6) Ehlerding, E. B.; Grodzinski, P.; Cai, W.; Liu, C. H. Big Potential from Small Agents: Nanoparticles for Imaging-Based Companion Diagnostics. *ACS Nano* **2018**, *12*, 2106-2121.

(7) Walsh, T. R.; Knecht, M. R. Biointerface Structural Effects on the Properties and Applications of Bioinspired Peptide-Based Nanomaterials. *Chem. Rev.* **2017**, *117*, 12641-12704.

(8) Ni, D.; Bu, W.; Ehlerding, E. B.; Cai, W.; Shi, J. Engineering of Inorganic Nanoparticles as Magnetic Resonance Imaging Contrast Agents. *Chem. Soc. Rev.* **2017**, *46*, 7438-7468.

(9) Chee, H. L.; Gan, C. R. R.; Ng, M.; Low, L.; Fernig, D. G.; Bhakoo, K. K.; Paramelle, D. Biocompatible Peptide-Coated Ultrasmall Superparamagnetic Iron Oxide Nanoparticles for In Vivo Contrast-Enhanced Magnetic Resonance Imaging. *ACS Nano* **2018**, *12*, 6480-6491.

(10) Zhan, N.; Palui, G.; Kapur, A.; Palomo, V.; Dawson, P. E.; Mattoussi, H. Controlling the Architecture, Coordination, and Reactivity of Nanoparticle Coating Utilizing an Amino Acid Central Scaffold, *J. Am. Chem. Soc.* **2015**, *137*, 16084-16097.

(11) Talamini, L.; Violatto, M. B.; Cai, Q.; Monopoli, M. P.; Kantner, K.; Krpetić, Ž.; Perez-Potti, A.; Cookman, J.; Garry, D.; Silveira, C. P.; Boselli, L.; Pelaz, B.; Serchi, T.; Cambier, S.; Gutleb, A. C.; Feliu, N.; Yan, Y.; Salmona, M.; Parak, W. J.; Dawson, K. A.; Bigini, P. Influence of Size and Shape on the Anatomical Distribution of Endotoxin-Free Gold Nanoparticles. *ACS Nano* **2017**, *11*, 5519-5529.

(12) Bergami, E.; Pugnalini, S.; Vannuccini, M. L.; Manfra, L.; Faleri, C.; Savorelli, F.; Dawson, K. A.; Corsi, I. Long-Term Toxicity of Surface-Charged Polystyrene Nanoplastics to Marine Planktonic Species *Dunaliella tertiolecta* and *Artemia franciscana. Aquat. Toxicol.* **2017**, *189*, 159-169.

(13) Burkett, S. L.; Read, M. J. Adsorption-Induced Conformational Changes of α-Helical Peptides. *Langmuir* **2001**, *17*, 5059-5065.

(14) Lynch, I.; Dawson, K. A.; Linse, S. Detecting Cryptic Epitopes Created by Nanoparticles. *Sci. STKE* **2006**, pe14.

(15) Lo Giudice, M. C.; Herda, L. M.; Polo, E.; Dawson, K. A. In Situ Characterization of Nanoparticle Biomolecular Interactions in Complex Biological Media by Flow Cytometry. *Nat. Commun.* **2016**, *7*, 13475.

(16) Herda, L. M.; Hristov, D. R.; Lo Giudice, M. C.; Polo, E.; Dawson, K. A. Mapping of Molecular Structure of the Nanoscale Surface in Bionanoparticles. *J. Am. Chem. Soc.* **2017**, *139*, 111-114.

(17) Kelly, P. M.; Åberg, C.; Polo, E.; O'Connell, A.; Cookman, J.; Fallon, J.; Krpetić, Z.; Dawson, K. A. Mapping Protein Binding Sites on the Biomolecular Corona of Nanoparticles. *Nat. Nanotechnol.* **2015**, *10*, 472-479.

(18) Castagnola, V.; Zhao, W.; Boselli, L.; Lo Giudice, M. C.; Meder, F.; Polo, E.; Paton, K. R.; Backes, C.; Coleman, J. N.; Dawson, K. A. Biological Recognition of Graphene Nanoflakes. *Nat. Commun.* **2018**, *9*, 1577.

(19) Xie, M.; Hansen, A. L.; Yuan, J.; Brüschweiler, R. Residue-Specific Interactions of an Intrinsically Disordered Protein with Silica Nanoparticles and Their Quantitative Prediction. *J. Phys. Chem. C* **2016**, *120*, 24463-24468.

(20) Hens, Z.; Martins, J. C. A Solution NMR Toolbox for Characterizing the Surface Chemistry of Colloidal Nanocrystals. *Chem. Mater.* **2013**, *25*, 1211-1221.

(21) Schönhoff, M. NMR Studies of Sorption and Adsorption Phenomena in Colloidal Systems. *Cur. Opin. Colloid In.* **2013**, *18*, 201-213.

(22) Ceccon, A.; Tugarinov, V.; Boughton, A. J.; Fushman, D.; Clore, G. M. Probing the Binding Modes of a Multidomain Protein to Lipid-based Nanoparticles by Relaxation-based NMR. *J. Phys. Chem. Lett.* **2017**, *8*, 2535-2540.

(23) Wang, A.; Perera, Y. R.; Davidson, M. B.; Fitzkee, N. C. Electrostatic Interactions and Protein Competition Reveal a Dynamic Surface in Gold Nanoparticle−Protein Adsorption. *J. Phys. Chem. C* **2016**, *120*, 24231-24239.

(24) Mayer, M.; Meyer, B. Characterization of Ligand Binding by Saturation Transfer Difference NMR Spectroscopy. *Angew. Chem., Int. Ed.* **1999,** *38*, 1784-1788.

(25) Mayer, M.; Meyer, B. Group Epitope Mapping by Saturation Transfer Difference NMR to Identify Segments of a Ligand in Direct Contact with a Protein Receptor. *J. Am. Chem. Soc.* **2001**, *123*, 6108-6117.

(26) Mayer, M.; James, T. L. NMR-Based Characterization of Phenothiazines as a RNA Binding Scaffold. *J. Am. Chem. Soc.* **2004**, *126*, 4453-4460

(27) Meyer, B.; Peters, T.; NMR Spectroscopy Techniques for Screening and Identifying Ligand Binding to Protein Receptors, *Angew. Chem. Int. Ed.* **2003**, *42*, 864-890.

(28) Blaum, B. S.; Neu, U.; Peters, T.; Stehle, T. Spin Ballet for Sweet Encounters: Saturation-Transfer Difference NMR and X-ray Crystallography Complement Each Other in the Elucidation of Protein–Glycan Interactions. *Acta. Cryst. F* **2018**, *74*, 451-462.

(29) Angulo, J.; Enriquez-Navas, P. M.; Nieto, P. M. Ligand–Receptor Binding Affinities from Saturation Transfer Difference (STD) NMR Spectroscopy: The Binding Isotherm of STD Initial Growth Rates. *Chem. Eur. J.* **2010**, *16*, 7803-7812.

(30) Zhang, Y.; Xu, H.; Parsons, A. M.; Casabianca, L. B. Examining Binding to Nanoparticle Surfaces Using Saturation Transfer Difference (STD)-NMR Spectroscopy. *J. Phys. Chem. C* **2017**, *121*, 24678-24686.

(31) Zhang, Y.; Xu, H.; Casabianca, L. B. Interaction Between Cyanine Dye IR-783 and Polystyrene Nanoparticles in Solution. *Magn. Reson. Chem.* **2018,** *56*, 1054-1060.

(32) Szczygiel, A.; Timmermans, L.; Fritzinger, B.; Martins, J. C. Widening the View on Dispersant-Pigment Interactions in Colloidal Dispersions with Saturation Transfer Difference NMR Spectroscopy. *J. Am. Chem. Soc.* **2009**, *131*, 17756-17758.

(33) Pitek, A. S.; O'Connell, D.; Mahon, E.; Monopoli, M. P.; Baldelli Bombelli, F.; Dawson, K. A. Transferrin Coated Nanoparticles: Study of the Bionano Interface in Human Plasma. *PLOS One* **2012**, *7*, e40685.

(34) Bramini, M.; Ye, D.; Hallerbach, A.; Raghnaill, M. N.; Salvati, A.; Åberg, C.; Dawson, K. A. Imaging Approach to Mechanistic Study of Nanoparticle Interactions with the Blood-Brain Barrier. *ACS Nano* **2014**, *8*,4304-4312.

(35) Kuhn, D. A.; Vanhecke, D.; Michen, B.; Blank, F.; Gehr, P.; Petri-Fink, A.; Rothen-Rutishauser, B. Different Endocytotic Uptake Mechanisms for Nanoparticles in Epithelial Cells and Macrophages. *Beilstein J. Nanotechnol*. **2014**, *5*, 1625-1636.

(36) Bergami, E.; Bocci, E.; Vannuccini, M. L.; Monopoli, M.; Salvati, A.; Dawson, K. A.; Corsi, I. Nano-Sized Polystyrene Affects Feeding, Behavior and Physiology of Brine Shrimp *Artemia franciscana* Larvae. *Ecotox. Environ. Safe*. **2016**, *123*, 18-25.

(37) Onorato, R. M.; Yoon, A. P.; Lin, J. T.; Somorjai, G. A. Adsorption of Amino Acids and Dipeptides to the Hydrophobic Polystyrene Interface Studied by SFG and QCM: The Special Case of Phenylalanine. *J. Phys. Chem. C* **2012**, *116*, 9947-9954.

(38) Hall, S. A.; Hickey, A. D.; Hore, D. K. Structure of Phenylalanine Adsorbed on Polystyrene from Nonlinear Vibrational Spectroscopy Measurements and Electronic Structure Calculations. *J. Phys. Chem. C* **2010**, *114*, 9748-9757.

(39) Jayalakshmi, V.; Krishna, N.; R. Complete Relaxation and Conformational Exchange Matrix (CORCEMA) Analysis of Intermolecular Saturation Transfer Effects in Reversibly Forming Ligand-Receptor Complexes. *J. Magn. Reson.* **2002**, *155*, 106-118.

(40) Angulo, J.; Nieto, P. M. STD-NMR: Application to Transient Interactions Between Biomolecules—A Quantitative Approach. *Eur. Biophys. J.* **2011**, *40*, 1357-1369.

(41) Hwang, T. L.; Shaka, A. J. Water Suppression That Works – Excitation Sculpting Using Arbitrary Wave-Forms and Pulsed-Field Gradients. *J. Magn. Reson. A* **1995**, *112*, 275-279.